

## Mechanism of 5,5-Dimethylhydantoin Chlorination: Monochlorination through a Dichloro Intermediate

Akin Akdag, S. D. Worley, Orlando Acevedo, and Michael L. McKee\*

*Department of Chemistry and Biochemistry, Auburn University,  
Auburn, Alabama 36849*

Received July 23, 2007

**Abstract:** The hydantoin moiety is an important pharmacore, and when halogenated, hydantoin derivatives act as excellent biocides. However, there have been no computational studies concerning the chlorination mechanism for the hydantoin moiety reported. Herein we describe a computational mechanistic study of the chlorination of 5,5-dimethylhydantoin (**H**) at the B3LYP/6-311+G(2d,p) level. Under a 1:1 molar ratio of hydantoin and a chlorinating agent (HOCl), conproportionation is calculated to be favorable to give the N1 monochloro derivative as the major predicted product, which is in agreement with experiment. Initial direct chlorination at the N1 position is prevented by a high kinetic barrier. The first step involves the deprotonation of the hydantoin moiety (at the N3 position) which is followed by a S<sub>N</sub>2 step transferring a chloronium ion (Cl<sup>+</sup>) from HOCl to the ionized hydantoin anion. A mechanism is proposed where the N3 nitrogen is chlorinated first followed by the N1 position to form the dichloro derivative. When CPCM solvation free energies ( $\Delta G(\text{solv})$ ) were added to the gas-phase free energies ( $\Delta G(\text{gas})$ ) along the S<sub>N</sub>2 reaction path, a sudden decrease in free energy was observed due to the incipient formation of the hydroxide ion. Explicit consideration of solvation within a box of 512 water molecules led to a much more gradual free energy change along the reaction path but a very similar free energy of activation.

### Introduction

The hydantoin (2,4-imidazolidinone) moiety is an important medicinal core unit.<sup>1</sup> As can be seen from the structure, it can be derivatized at several positions. Substitution of the hydrogens on the ring with various organic groups has led to hydantoin based drugs,<sup>2</sup> e.g. 5,5-diphenylhydantoin and 5-ethyl-1-methyl-5-phenylhydantoin (Figure 1). The quest for hydantoin-based drugs remains in progress.<sup>3</sup>

Another hydantoin derivative is 5,5-dimethylhydantoin (**H**) whose chlorinated and brominated derivatives have been used both as biocides and organic reagents.<sup>4</sup> Halogenated **H** and similar heterocyclic ring compounds (see Figure 2 for the chlorinated **H** derivatives) have been employed as biocidal moieties in antimicrobial materials in these laboratories.<sup>5</sup> For example, 5,5-dimethyl-3-[3-(triethoxysilyl)propyl]hydantoin (Figure 2) has been shown to be a versatile biocide precursor

and can easily be coated onto hard and soft surfaces,<sup>6</sup> and the halogenated derivatives of polystyrene hydantoin beads are being employed in developing countries for disinfecting water.<sup>5c</sup>

In previous work, we have studied the stabilities and the mechanism of formation of the N–Cl bond in different heterocyclic moieties<sup>7</sup> and showed that the nature of the substitution around the nitrogen is important for N–Cl bond stability. Moreover, the stability order N–Cl(amine) > N–Cl(amide) > N–Cl(imide) was predicted, which was in accord with experimental observations.<sup>8</sup> Despite the usefulness of these compounds, no computational reports have been published concerning the mechanism of the halogenation of the hydantoin ring moiety. In very interesting early experimental studies concerning halogenation of hydantoin derivatives, it was shown that the thermodynamically controlled monohalogenation product was that containing halogen at the amide nitrogen N1 (Figure 2).<sup>9</sup> A mechanism was

\* Corresponding author e-mail: mckee@chem.auburn.edu.

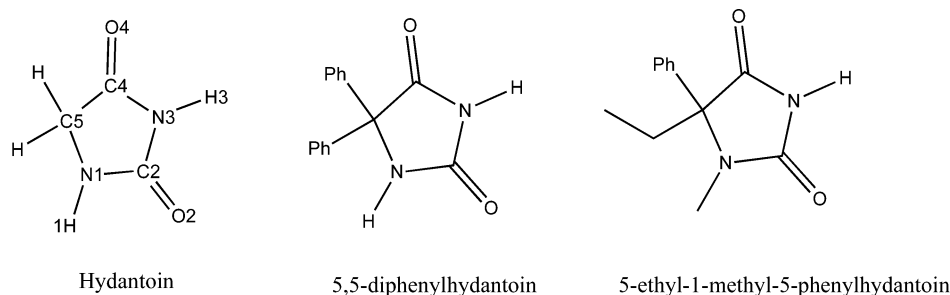


**Figure 1.** Structure of the hydantoin ring and its numbering system. Two examples of important medicinal hydantoin derivatives.

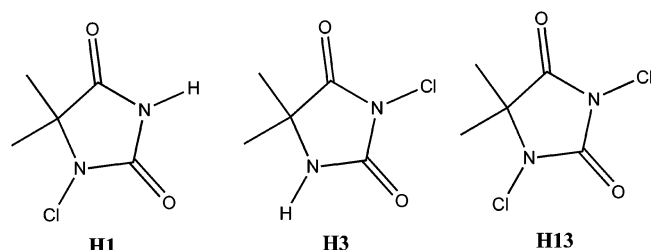
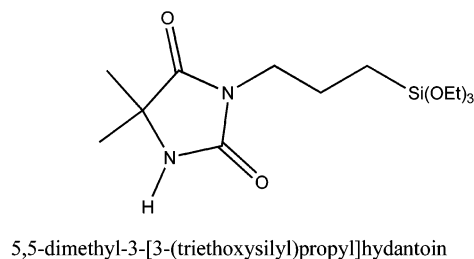


**Figure 2.** An example of a precursor of a biocidal hydantoin derivative and halogenated 5,5-dimethylhydantoin derivatives.

proposed in which the 1,3-dihalogenated intermediate transferred halogen from the imide nitrogen to the amide nitrogen on an unhalogenated hydantoin molecule.<sup>9</sup>

In this article chlorination of 5,5-dimethylhydantoin was investigated at the B3LYP/6-311+G(2d,p) level. The chlorination of the hydantoin required a two-step process: prechlorination (acid–base equilibrium) and chlorination. Each of these steps was studied computationally with solvation effects included.

## Computational Methods

All electronic structure calculations were performed with Gaussian03.<sup>10</sup> The structures were optimized, and zero-point and thermal corrections were calculated at the B3LYP/6-311+G(2d,p) level. Solvation effects were included on the geometry obtained at the B3LYP/6-311+G(2d,p) level with CPCM and tesserae set to 0.05 Å.<sup>2</sup> In the conductor-like polarizable continuum model (CPCM),<sup>12</sup> the solute molecule is placed into a cavity surrounded by the solvent considered as a continuum medium with a dielectric constant of 78.39 (water). The charge distribution of the solute polarizes the dielectric continuum, which creates an electrostatic field that in turn polarizes the solute. In specifying the molecular cavity, the United Atom Topological Model was used with radii optimized for the PBE0/6-31G(d) level of theory (i.e., RADII=UAKS). The choice of UAKS radii was shown by

Houk and co-workers<sup>11</sup> to give good results for anions. The aqueous free energies were computed using eq 1.

$$\Delta G(\text{aq}) = \Delta G(\text{gas}) + \Delta G(\text{solvation}) \quad (1)$$

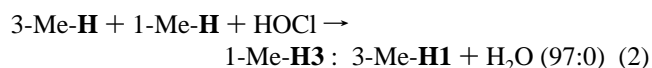
A 1.9 kcal/mol correction was included in the calculation due to the fact that the molecules are changing in state from ideal gas to ideal solution. A correction shift of 2.4 kcal/mol was also applied to H<sub>2</sub>O due to the fact that the water molarity is 55.56.<sup>13</sup> Experimental free energies of solvation were used for H<sub>3</sub>O<sup>+</sup> (−110.2 kcal/mol) and OH<sup>−</sup> (−104.6 kcal/mol).<sup>14</sup>

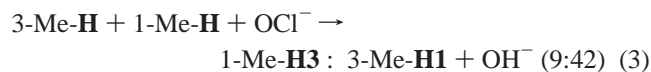
Explicit consideration of solvation<sup>15</sup> was made by using the BOSS program.<sup>16</sup> The solvent molecules were represented by the TIP4P water model<sup>17</sup> in a periodic box of 512 (minus the number of non-hydrogen atoms of the solute) water molecules at 25 °C and 1 atm in the NPT ensemble.<sup>18</sup> Each simulation consisted of 5 million configurations of equilibration and 10 million configurations of averaging. The solute energy and energy changes were treated quantum mechanically using PDDG/PM3<sup>19</sup> where the partial charges were obtained from the CM3 charge model,<sup>20</sup> unscaled for negatively charged solutes or scaled by 1.14 for neutral charged solutes<sup>21</sup> with solute–solvent and solvent–solvent intermolecular cutoff distances of 10 Å. This method is particularly well suited for the study of S<sub>N</sub>2 reactions.<sup>22</sup>

The labeling used in this work indicates the location of the chlorine atom(s) and the location of the labile hydrogen atom(s). For example, **H** is the parent hydantoin (5,5-dimethylhydantoin) and **H3** is the 3-chloro derivative, **H-an1** is the anion formed by removing the proton attached to N1, and **H1-an3** is the 1-chloro derivative of **H** with a proton removed from N3. Likewise, **H-12t** is the tautomer of **H** with labile hydrogens at N1 and O2, and **H1-4t** is the tautomer of the 1-chloro derivative of **H** with hydrogens at N3 and O4. Occasional use is made of notations such as 1-Me-**H** and 1-Me-**H3** which are 1,5,5-trimethylhydantoin and 3-chloro-1,5,5-trimethylhydantoin, respectively.

## Results and Discussion

When Corral and Orazi studied<sup>9</sup> the competitive chlorination of 3,5,5-trimethylhydantoin/1,5,5-trimethylhydantoin with HOCl (eq 2), they found the ratio of 3-chloro-1,5,5-trimethylhydantoin:1-chloro-3,5,5-trimethylhydantoin to be 97:0. When the chlorination agent was changed to be OCl<sup>−</sup>, the ratio became 9:42 (eq 3).





This result indicates that two major products are possible. The work below will support the hypothesis that the **H1** product is the thermodynamic product, and **H3** is the kinetic product. In addition to the chlorinating agents HOCl and  $\text{OCl}^-$ , 1-Me-**H3** (3-chloro-1,5,5-trimethylhydantoin) could also act as a chlorinating agent (eq 4) at the N1 position. In acetone (eq 5), the dichloro derivative **H13** directs 100% chlorination of **H** at the N1 position (forming **H1**).



This conproportionation reaction suggests that the N1 position can be favored over the N3 position as the final site of chlorination. The main objective of this article is to account for the observed monochlorination of **H** (under equal hydantoin:HOCl molar ratio) at the N1 position to form the thermodynamically controlled product even though the N3 position provides the kinetically controlled product. A plausible chlorination mechanism begins with ionization, followed by an  $\text{S}_{\text{N}}2$  transfer of a chloronium ion ( $\text{Cl}^+$ ) to the nitrogen. Another possibility is the tautomerization of the hydantoin to another form which is more reactive than the hydantoin itself.

**Tautomers and Ionization.** For an illustration of the formation of various tautomers<sup>23</sup> see Schemes 1 and 2.

Relative energies of hydantoin tautomers are given in Table 1, while relative energies of species in the chlorination mechanism are given in Table 2. As seen in Table 2, the

**Table 1.** Relative Enthalpies and Free Energies (kcal/mol) Tautomers of **H**, **H3**, and **H1**<sup>a</sup>

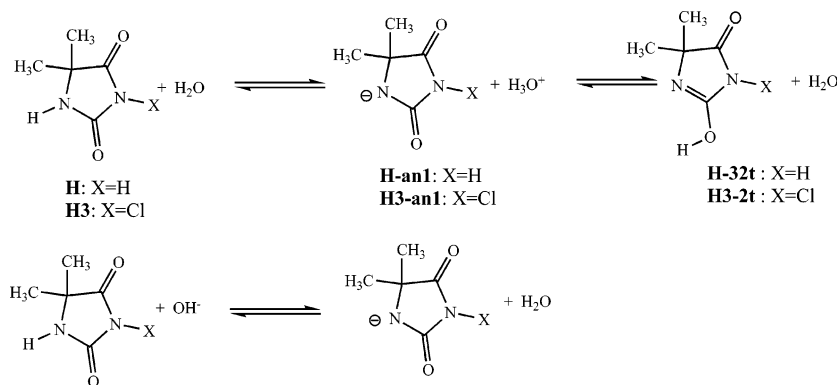
	$\Delta H$ (0K)	$\Delta H$ (g,298K)	$\Delta G$ (g,298K)	$\Delta G$ (aq,298K)
<b>H</b>	0.0	0.0	0.0	0.0
<b>H-32t</b>	17.3	17.7	20.4	22.3
<b>H-12t</b>	18.7	19.0	21.7	18.1
<b>H-14t</b>	18.0	18.4	20.8	18.0
<b>H3</b>	0.0	0.0	0.0	0.0
<b>H3-2t</b>	16.9	16.8	16.3	19.4
<b>H1</b>	-1.1	-1.2	-2.0	-3.9
<b>H1-2t</b>	17.4	17.2	15.6	15.2
<b>H1-4t</b>	15.3	16.3	13.5	11.8

<sup>a</sup> The labeling indicates the location of the chlorine atom and the location of the labile hydrogen atom(s) in the tautomer. For example, **H** is the parent 5,5-dimethylhydantoin, and **H3** is the 3-chloro derivative; **H-12t** is the tautomer of **H** with labile hydrogens at the N1 and O2 positions, while **H1-4t** is the tautomer of the 1-chloro derivative with hydrogen at the O4 position.

ionization of the amide (**H**  $\rightarrow$  **H-an1**) requires 27.6 kcal/mol of free energy which is 5.3 kcal/mol higher than that of the corresponding tautomer (**H**  $\rightarrow$  **H-32t**). Therefore, the ionized hydantoin **H-an1** is predicted to be in equilibrium with **H** and **H-32t**. It was found that if the hydantoin is chlorinated at N3 (**H3**), then the deprotonation (**H3**  $\rightarrow$  **H3-an1**) is 8.0 kcal/mol more spontaneous than the corresponding unchlorinated derivative (**H**  $\rightarrow$  **H-an1**, see Table 2).

This can be attributed to the fact that chlorine is withdrawing electron density since it has partial positive charge (the natural charge, i.e., NPA charge on Cl is 0.14), i.e. the proton bonded to the N3 moiety is more acidic than is the proton bonded to N1. The  $\text{pK}_{\text{a}}$  and free energies changes of several relevant hydantions<sup>1</sup> are tabulated in Table 3. The  $\text{pK}_{\text{a}}$  of **H**

**Scheme 1.** Dissociation of **H** and **H3** under Neutral and Basic Conditions



**Scheme 2.** Dissociation of **H** and **H1** under Neutral and Basic Conditions

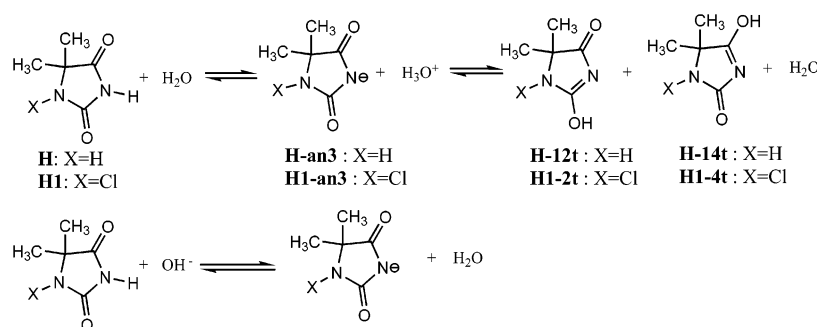


**Table 2.** Enthalpies and Free Energies for the Chlorination Step of 5,5-Dimethylhydantoin (**H**) by HOCl

		$\Delta H$ (0K)	$\Delta H$ (g,298K)	$\Delta G$ (g,298K)	$\Delta G$ (aq,298K)	adj. $\Delta G^a$ (aq,298K)
<b>a</b>	<b>H</b> + 2H <sub>2</sub> O + 2HOCl	0.0	0.0	0.0	0.0	0.0
<b>b</b>	<b>H-an3</b> + H <sub>2</sub> O + 2HOCl + H <sub>3</sub> O <sup>+</sup>	178.9	179.0	179.2	18.6	18.6
<b>c</b>	<b>H3</b> + H <sub>2</sub> O + HOCl + H <sub>3</sub> O <sup>+</sup> + OH <sup>-</sup>	214.5	215.4	210.8	9.3	-9.8
<b>d</b>	<b>H3-an1</b> + HOCl + 2H <sub>3</sub> O <sup>+</sup> + OH <sup>-</sup>	389.0	389.7	383.5	28.9	9.8
<b>e</b>	<b>H13</b> + 2H <sub>3</sub> O <sup>+</sup> + 2OH <sup>-</sup>	428.1	429.4	416.4	16.4	-21.8
<b>f</b>	<b>H-an1</b> + H <sub>2</sub> O + 2HOCl + H <sub>3</sub> O <sup>+</sup>	183.8	184.0	185.4	27.6	27.6
<b>g</b>	<b>H1</b> + H <sub>2</sub> O + HOCl + H <sub>3</sub> O <sup>+</sup> + OH <sup>-</sup>	213.4	214.2	208.8	5.4	-13.7
<b>h</b>	<b>H1-an3</b> + HOCl + 2H <sub>3</sub> O <sup>+</sup> + OH <sup>-</sup>	382.2	382.8	374.6	20.8	1.7
<b>i</b>	<b>H-an3</b> + HOCl → <b>H3</b> + OH <sup>-</sup> <sup>b</sup>	35.6	36.4	31.6	-9.3	-28.4
<b>j</b>	<b>H-an3</b> + <b>H13</b> → <b>H3</b> + <b>H1-an3</b> <sup>c</sup>	-10.3	-10.2	-10.2	-4.9	-4.9
<b>k</b>	<b>H</b> + <b>H13</b> → 2 <b>H1</b> <sup>d</sup>	-1.3	-1.0	1.2	-5.6	-5.6
<b>l</b>	<b>H</b> + <b>H13</b> → 2 <b>H3</b> <sup>e</sup>	0.9	1.4	5.2	2.2	2.2

<sup>a</sup> The free energy has been reduced by 19.1 kcal/mol for each (H<sub>3</sub>O<sup>+</sup>/OH<sup>-</sup>) pair which is the experimental free energy change for H<sub>3</sub>O<sup>+</sup>(aq) + OH<sup>-</sup>(aq) → 2H<sub>2</sub>O(l). The calculated value for this process is 20.1 kcal/mol. <sup>b</sup> Reaction thermochemistry is equivalent to -**b**+**c**. <sup>c</sup> Reaction thermochemistry is equivalent to -**b**-**e**+**c**+**h**. <sup>d</sup> Reaction thermochemistry is equivalent to -**a**-**e**+2**g**. <sup>e</sup> Reaction thermochemistry is equivalent to -**a**-**e**+2**c**.

**Table 3.** Experimental and Calculated Free Energy Changes (kcal/mol) for Ionization in Hydantoins

hydantoin (ionization)	site of ionization	pK <sub>a</sub> <sup>a</sup>	exptl $\Delta G^b$	calc $\Delta G$	difference
5,5-dimethyl ( <b>H</b> → <b>H-an3</b> )	N3	9.03	14.7	18.6	3.9
1,5,5-trimethyl ( <b>H</b> → <b>H-an3</b> ) <sup>c</sup>	N3	9.02	14.7	18.6	3.9
3,5,5-trimethyl ( <b>H</b> → <b>H-an1</b> ) <sup>c</sup>	N1	>14	>21.5	27.6	<6.1
1-chloro-5,5-dimethyl ( <b>H1</b> → <b>H1-an3</b> )	N3	7.17	12.2	15.4	3.2

<sup>a</sup> Reference 9. <sup>b</sup>  $\Delta G = -RT \ln K_a + 2.4$  kcal/mol (correction, see ref 24). <sup>c</sup> The effect of the methyl group at the N1 or the N3 position is assumed to be small relative to a hydrogen atom.

is 9.03<sup>24</sup> which is only slightly changed if the N1 position is methylated (9.02). On the other hand, if the N3 position is methylated, the pK<sub>a</sub> is 14 or greater. Chlorination of **H** at the N1 position makes the hydantoin more acidic (pK<sub>a</sub>=7.17). The experimental free energy changes computed from the pK<sub>a</sub> values are in good agreement with the calculated free energy changes (Table 3).

**S<sub>N</sub>2 Chlorination.** **H-an3** is thermodynamically favored over **H-an1** by 9.0 kcal/mol. The negative charge on nitrogen makes N3 nucleophilic such that it can react with hypochlorous acid in an S<sub>N</sub>2 reaction to produce **H3** and hydroxide. Attempts to locate a transition state in the gas phase at the B3LYP/6-311+G(2d,p) level for the **H-an3** + HOCl → **H3** + OH<sup>-</sup> S<sub>N</sub>2 reaction failed. The problem is due to the poor representation of the aqueous free energy surface using gas-phase optimizations. At 298 K, the gas-phase enthalpy of reaction is +36.4 kcal/mol, while the aqueous phase free energy difference is -28.4 kcal/mol (Table 2), a 64.8 kcal/mol difference! The gas-phase potential energy surface is dominated by the ion-molecule complex **H-an3-complex**, 13.5 kcal/mol more stable than **H-an3** + HOCl, with N-Cl and O-Cl distances of 2.26 and 1.85 Å, respectively. When eq 1 is applied to **H-an3-complex**, the free energy is 6.8 kcal/mol higher than **H-an3** + HOCl. The aqueous-phase destabilization is due to charge delocalization in the complex which has a free energy of solvation 9.8 kcal/mol smaller than **H-an3** + HOCl (Table S3).

While the ion-molecule complex **H-an3-complex** is a minimum in the gas phase, it may be close to the maximum along the aqueous S<sub>N</sub>2 free energy reaction profile. To address this issue we have calculated a reaction path **H-an3** + HOCl → **H3** + OH<sup>-</sup> by varying the Cl-OH distance from

1.85 (RC185) to 2.70 (RC270) Å in steps of 0.05 Å. The structures were fully optimized at the B3LYP/6-311+G(2d,p) level, and frequencies were computed after projecting out the reaction coordinate.<sup>25</sup> Solvation energies were computed using the CPCM solvation model and UAKS radii (see Tables S2 and S3). The results are plotted in Figure 3.

While the contribution of zero-point correction, heat capacity correction, and entropy to  $\Delta G$ (aq) were constant to about 1 kcal/mol along the **H-an3** chlorination reaction path (Table S3), the interaction energies become more positive (less binding) systematically, from -13.5 to 9.8 kcal/mol. At the same time, the solvation free energy  $\Delta G$ (solv) becomes more negative (-67.8 to -99.1 kcal/mol) which is due to the emergence of a strongly solvated hydroxide anion. The majority of the decrease occurs from RC215 to RC 220 where there is a 13.2 kcal/mol drop in  $\Delta G$ (solv). Adding  $\Delta G$ (g) and  $\Delta G$ (solv) to give  $\Delta G$ (aq) gives a maximum in the free energy curve at RC215 which is 9.9 kcal/mol above **H-an3** + HOCl.

The reaction path for **H-an1** + HOCl → **H1** + OH<sup>-</sup>, also shown in Figure 3, has a free energy barrier of 5.8 kcal/mol. The plots of both reactions are relative to separated reactants, but we note that **H-an3** is 9.0 kcal/mol lower (more spontaneous) than **H-an1** (Table 2). Thus, even though chlorination of **H-an1** has a lower free energy barrier than **H-an3**, the overall process, including ionization, is higher (27.6 + 5.8 = 33.4 for **H-an1** versus 18.6 + 9.9 = 28.5 kcal/mol for **H-an3**).

To determine the cause of the discontinuity in free energy, we plotted the NPA charge of the OH group as a function of the **H-an3** + HOCl → **H3** + OH<sup>-</sup> reaction coordinate (Figure 4). The charge of the OH group in the gas phase



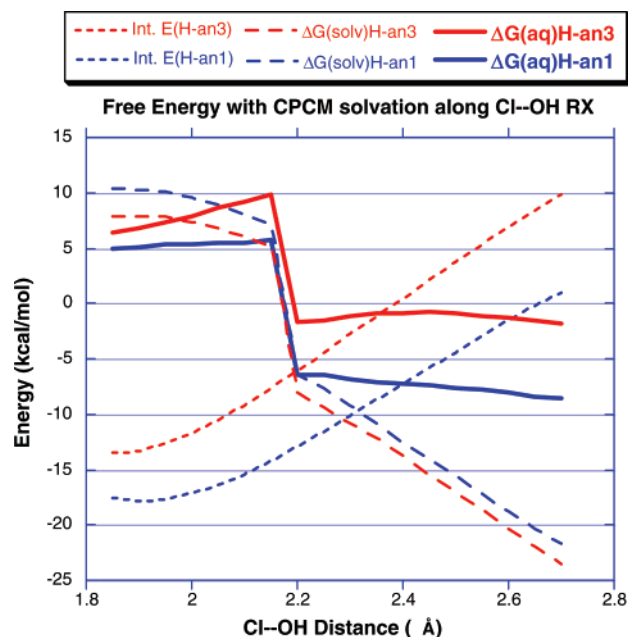


**Figure 3.** Plot of the electronic interaction energy (Int) between **H-an3/H-an1** and HOCl (red/blue upward dashed curves), the solvation free energy  $\Delta G(\text{solv})$  (red/blue downward dashed curves), and the aqueous free energy  $\Delta G(\text{aq})$  (red/blue solid curves) along the reaction coordinate in the reaction **H-an3** + HOCl  $\rightarrow$  **H3** + OH<sup>-</sup> (red lines) and **H-an1** + HOCl  $\rightarrow$  **H1** + OH<sup>-</sup> (blue lines).

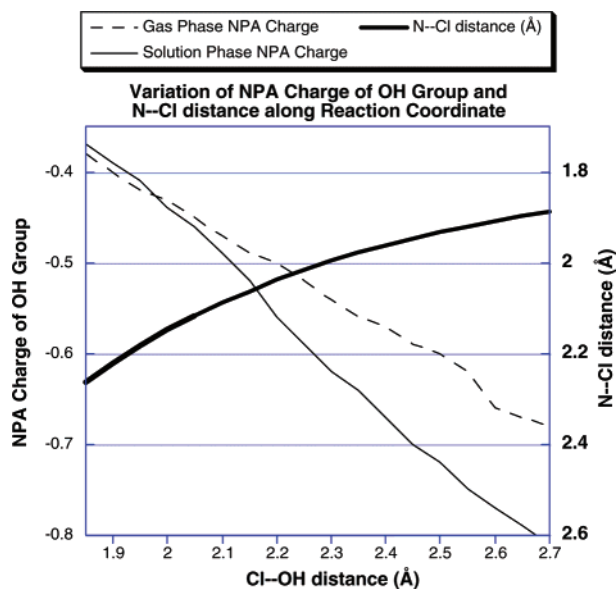


**Figure 4.** Plot of NPA charges for H group and N-Cl distance as a function of the Cl-OH reaction coordinate in the reaction **H-an3** + HOCl  $\rightarrow$  **H3** + OH<sup>-</sup>.

and the solution phase both increase as Cl-OH distances increase. The larger increase in solution phase reflects the greater polarizing ability of the environment. However, there is no abrupt change in the OH group charge. In addition, the N-Cl distance smoothly decreases as the Cl-OH distance increases. The discontinuity is caused by a change in the assigned radius of oxygen as the Cl-OH distances increases. Thus, the contribution of  $\Delta G_{\text{el}}$ , the solvation free energy due to electrostatic interactions, to the CPCM

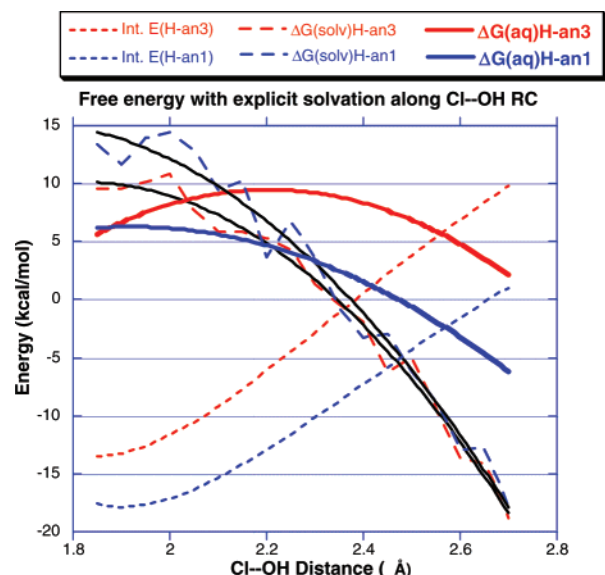


**Figure 5.** Plot of electronic interaction energy (Int) between **H-an3/H-an1** and HOCl (kcal/mol), the solvation free energy  $\Delta G(\text{solv})$ , and the aqueous free energy  $\Delta G(\text{aq})$  along the reaction coordinate in the reaction **H-an3** + HOCl  $\rightarrow$  **H3** + OH<sup>-</sup> (red dashed/solid lines) and **H-an1** + HOCl  $\rightarrow$  **H1** + OH<sup>-</sup> (blue dashed/solid lines).

solvation free energy shows a discontinuous change along the reaction coordinate between a Cl-OH distance of 2.15 and 2.20 Å. For a Cl-OH distance of 2.15 Å (and less), the program uses an atomic radius of 1.563 Å for the oxygen atom of the OH group, while for a Cl-OH distance of 2.20 Å (and greater), the program uses an atomic radius of 1.290 Å.

The very dramatic increase in solvation free energy between RC215 and RC220 is unusual and may be an artifact of using the CPCM method. Therefore, we considered an alternative way of computing solvation along the reaction path. Each structure along the reaction coordinate was equilibrated (5 M steps) and averaged (10 M steps) in a box of 512 water molecules. The variations of  $\Delta G(\text{solv})$  and  $\Delta G(\text{aq})$  from explicit solvation for the chlorination of **H-an3** and **H-an1** are given in Figure 5 and Tables S2 and S3.

The solvation free energy becomes more negative as the reaction proceeds. The variation of solvation free energy at the 18 individual points along the reaction path is superimposed on the fitted quadratic line. The reference energy is **H-an3** + HOCl (red lines) or **H-an1** + HOCl (blue lines).

The overall trend in the increase (more negative) of  $\Delta G(\text{solv})$  along the reaction path is the same as that obtained with the CPCM method. However, the position in the maximum in  $\Delta G(\text{aq})$  is displaced later ( $\Delta G^\ddagger \approx 9$  kcal/mol at about 2.3 Å) for the chlorination of **H-an3** and earlier for the chlorination of **H-an1** ( $\Delta G^\ddagger \approx 6$  kcal/mol at about 1.9 Å) relative to the maximum in  $\Delta G(\text{aq})$  from the CPCM method (Figures 3 and 5). In addition, the variation of the fitted  $\Delta G(\text{solv})$  and  $\Delta G(\text{aq})$  for explicit solvation is much smoother along the reaction path than for CPCM.

The solvation effect with the CPCM method is from the solute embedded in a cavity and the interaction between the

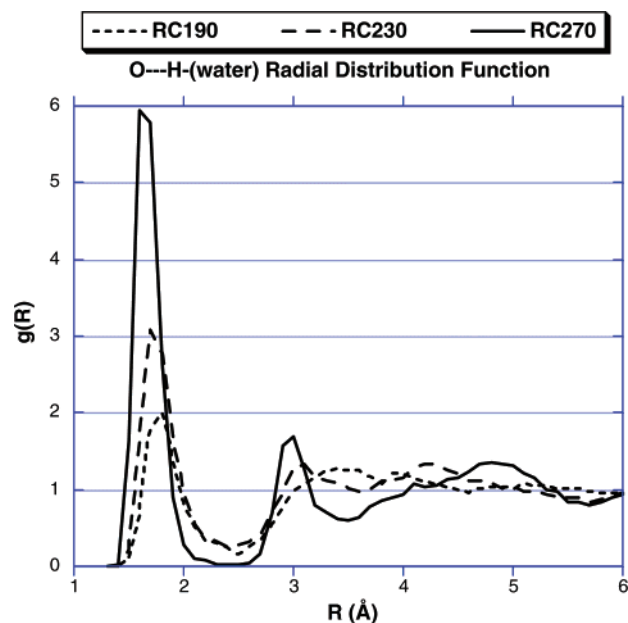


**Figure 6.** Radial distribution function  $g(R)$  for the O—H(water) distances for three structures along the reaction coordinate in the reaction  $\mathbf{H-an3} + \text{ClOH} \rightarrow \mathbf{H3} + \text{OH}^-$ .

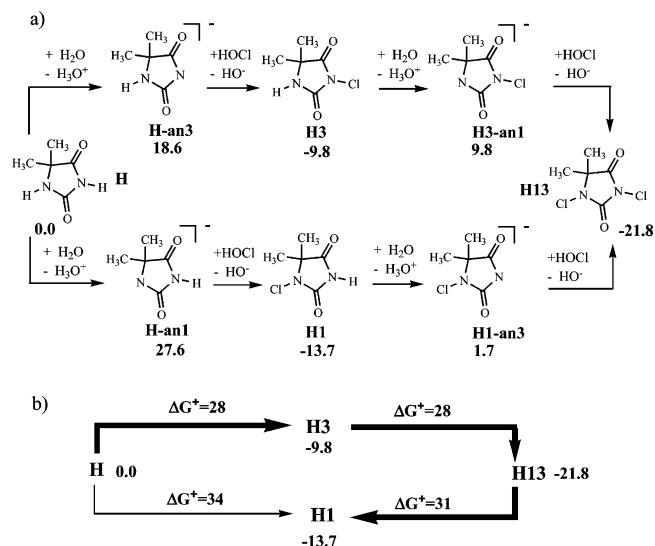
solute and the solvent dielectric at the cavity surface. In explicit solvation, the accessibility of the solute to the solvent is more realistically modeled. As the hydroxide ion departs along the reaction path, the water molecules adopt a very tight solvation shell. This is illustrated in the radial distribution function (Figure 6) for the chlorination of  $\mathbf{H-an3}$  at three points along the reaction path, RC190, RC230, and RC270 which represent points before, near, and after the maximum in  $\Delta G(\text{aq})$ .

At the last point, RC270, a very sharp peak in the distribution between the oxygen of the developing OH and the hydrogens of water is apparent at about 1.7 Å with a strong secondary solvent shell at 3.0 Å. At earlier points (RC230 and RC190), there is a gradual decrease in the size of the peak and a movement to a larger O—H separation.

With these results in hand, a summary of relative free energies is given in Figure 7.

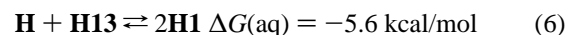
After monochlorination of the hydantoin occurs, the monochlorinated hydantoin can deprotonate. Therefore, the same argument is valid for the addition of second chlorine to the hydantoin in an  $\text{S}_{\text{N}}2$ -like reaction mechanism. The values of  $\Delta G^\ddagger$  for the  $\mathbf{H3} \rightarrow \mathbf{H13}$  step (28 kcal/mol) and the  $\mathbf{H13} \rightarrow \mathbf{H1}$  step (31 kcal/mol) in Figure 7b are estimated by assuming that the chlorination step has a 8 kcal/mol barrier. For  $\mathbf{H3} \rightarrow \mathbf{H13}$ , this is  $\mathbf{H3} \rightarrow \mathbf{H3-an1}$  (19.6 kcal/mol) plus 8 kcal/mol. For  $\mathbf{H13} \rightarrow \mathbf{H1}$ , the barrier for the reverse reaction  $\mathbf{H1} \rightarrow \mathbf{H13}$  (i.e.,  $\mathbf{H1} \rightarrow \mathbf{H1-an3}$  (15.4 kcal/mol) + 8) is added to the free energy of the reaction ( $-13.7 + 21.8 = 8.1$  kcal/mol) to give an estimated free energy barrier of (15.4 + 8 + 8.1) 31.5 kcal/mol for the forward reaction.

Table 2 shows that the formation of  $\mathbf{H13}$  from  $\mathbf{H1-an3}$  is less favored than that from  $\mathbf{H3-an1}$  energetically. This can be attributed to fact that the thermodynamic stability of the amide N—Cl bond is higher than for the imide N—Cl bond. The high negative charge is localized on N3 relative to N1.  $\mathbf{H1}$  is favored over  $\mathbf{H3}$  by 1.2 kcal/mol at  $\Delta H(\text{g}, 298\text{K})$ . The



**Figure 7.** The most favorable path to  $\mathbf{H1}$  is  $\mathbf{H} \rightarrow \mathbf{H3} \rightarrow \mathbf{H13} \rightarrow \mathbf{H1}$ . (a) Aqueous free energies (kcal/mol) of species relative to  $\mathbf{H} + 2\text{H}_2\text{O} + 2\text{HOCl}$ . (b) Aqueous free energies (kcal/mol) of species along the chlorination reaction path. The values  $\Delta G^\ddagger$  are relative free energies with respect to the indicated reactant.

stability is increased to 3.9 kcal/mol for  $\Delta G(\text{aq}, 298\text{K})$ . Hypochlorous acid is a much better chlorinating agent than  $\mathbf{H13}$  as shown by reaction **i** (Table 2) which is 28.4 kcal/mol spontaneous compared to reaction **j** which is 4.9 kcal/mol spontaneous. However, under a 1:1 equal molar ratio of  $\mathbf{H}$  to HOCl, HOCl will be exhausted after one-half of  $\mathbf{H}$  is converted into  $\mathbf{H13}$ . Thus, under conditions of limited chlorinating agent, the reaction will be thermodynamically driven to monochlorination at the N1 position (eq 6 and reaction **k**, Table 2). Under conditions of excess chlorination agent, the dichlorohydantoin derivative is expected.



## Conclusions

In this study we have investigated a plausible mechanism for the chlorination of 5,5-dimethylhydantoin. The mechanism was broken into two parts: (1) prechlorination (acid–base equilibrium) and (2) chlorination. The dissociation of a proton from N3 is calculated to be more favorable than from N1, in agreement with experimental observations. When monochlorinated, the hydantoin become significantly more acidic.

The chlorination step was investigated in an  $\text{S}_{\text{N}}2$ -like mechanism, in which the anions act as nucleophiles and hydroxide as a leaving group. Since the N—Cl bond is stronger than the O—Cl bond thermodynamically, this reaction is favored. Moreover, the hydroxide anion has significantly more solvation free energy than the corresponding hydantoin anion derivatives. Based upon the prechlorination step,  $\mathbf{H3}$  is favored kinetically. On the other hand, chlorination stabilizes  $\mathbf{H1}$  over  $\mathbf{H3}$ . The preferred route of chlorination is to form  $\mathbf{H3}$  (monochlorination) and then  $\mathbf{H13}$  (dichlorination). If limited chlorination agent is used, the conproportionation reaction  $\mathbf{H} + \mathbf{H13} \rightleftharpoons 2\mathbf{H1}$  can take place to produce  $\mathbf{H1}$  (monochlorination) as the thermodynamically

avored product. Thus, the computations reported herein support the mechanism suggested for **H1** formation in the experimental paper by Corral and Orazi.<sup>9</sup> They also demonstrate the utility of such computations in the study of important complex organic reactions.

**Acknowledgment.** This work has been supported by the U.S. Air Force through contract F08637-02-C-7020 and the Vanson HaloSource Company. The computation time was provided by Auburn University and the Alabama supercomputer.

**Supporting Information Available:** Absolute energies, zero-point energies, enthalpy corrections, entropies, and solvation energies for various species (Table S1); absolute energies, zero-point energies, enthalpy corrections, entropies, and solvation energies (CPCM and explicit) for points along the  $S_N2$  reaction path for the chlorination of **H-an3** and **H-an1** (Tables S2 and S3); the full citation for ref 10; and optimized Cartesian coordinates of all related species at the B3LYP/6-311+G(2d,p) level (Table S4). This material is available free of charge via the Internet at <http://pubs.acs.org>.

## References

- (1) Avendaño, C.; Menendez, J. C. *Hydantoin and Its Derivatives*. In *Kirk-Othmer Encyclopedia Chemical Technology*, 4th ed.; 2000; pp 1–21. (DOI:10.1002/0471238961.0825040101220514.a01).
- (2) Meusel, M.; Gütschow, M. *Org. Preparations Procedures Int.* **2004**, 36, 391–443.
- (3) (a) Kruger, H. G.; Mdluli, P. S. *Struct. Chem.* **2006**, 17, 121–125. (b) Teng, X.; Degterev, A.; Jagtap, P.; Xing, X.; Choi, S.; Denu, R.; Yuan, J.; Cuny, G. D. *Bioorg. Med. Chem. Lett.* **2005**, 15, 5039–5044. (c) Riley, P.; Figary, P. C.; Entwisle, J. R.; Roe, A. L.; Thompson, G. A.; Ohashi, R.; Ohashi, N.; Moorehead, T. J. *J. Pharm. Sci.* **2005**, 94, 2084–2095. (d) Wehner, V.; Stiltz, H.-U.; Osipov, S. N.; Golubev, A. S.; Sieler, J.; Burger, K. *Tetrahedron* **2004**, 60, 4295–4302. (e) Bakalova, A.; Buyukliev, R.; Momekov, G.; Ivanov, D.; Todorov, D.; Konstantinov, S.; Karaivanova, M. *Eur. J. Med. Chem.* **2005**, 40, 590–596. (f) Krishnan, R. S. G.; Thennarasu, S.; Mandal, A. B. *Chem. Phys.* **2003**, 291, 195–205.
- (4) (a) Akdag, A.; Webb, T.; Worley, S. D. *Tetrahedron Lett.* **2006**, 47, 3509–3510. (b) Walters, T. R.; Zajac, W. W.; Woods, J. M. *J. Org. Chem.* **1991**, 56, 316–321. (c) Szumigala, R. H.; Devine, P. N.; Gauthier, D. R.; Volante, R. P. *J. Org. Chem.* **2004**, 69, 566–569. (d) Rivera, N. R.; Balsells, J.; Hansen, K. B. *Tetrahedron Lett.* **2006**, 47, 4889–4891. (e) Bartoli, G.; Bosco, M.; Carlone, A.; Locatelli, M.; Melchiorre, P.; Sambri, L. *Angew. Chem., Int. Ed.* **2005**, 44, 6219–6222. (f) Soracco, R. J.; Wilde, E. W.; Mayack, L. A.; Pope, D. H. *Water Res.* **1985**, 19, 763–766. (g) Koval, I. V. *Russ. J. Org. Chem.* **2001**, 37, 297–317.
- (5) (a) Tsao, T. C.; Williams, D. E.; Worley, C. G.; Worley, S. D. *Biotechnol. Prog.* **1991**, 7, 60–66. (b) Chen, Y.; Worley, S. D.; Kim, J.; Wei, C.-I.; Chen, T.-Y.; Suess, J.; Kawai, H.; Williams, J. F. *Ind. Eng. Chem. Res.* **2003**, 42, 5715–5720. (c) Worley, S. D.; Sun, G. *Trends Polym. Sci.* **1996**, 4, 364–370.
- (6) (a) Liang, J.; Owens, J. R.; Huang, T. S.; Worley, S. D. *J. Appl. Polym. Sci.* **2006**, 101, 3448–3454. (b) Liang, J.; Wu, R.; Huang, T. S.; Worley, S. D. *J. Appl. Polym. Sci.* **2005**, 97, 1161–1166.
- (7) (a) Akdag, A.; Okur, S.; McKee, M. L.; Worley, S. D. *J. Chem. Theory Comput.* **2006**, 2, 879–884. (b) Akdag, A.; McKee, M. L.; Worley, S. D. *J. Phys. Chem. A* **2006**, 110, 7621–7627.
- (8) Qian, L.; Sun, G. *J. Appl. Polym. Sci.* **2003**, 89, 2418–2425, and references cited therein.
- (9) (a) Corral, R. A.; Orazi, O. O. *J. Org. Chem.* **1963**, 28, 1100–1104. (b) Petterson, R. C.; Grzeskowiak, U. *J. Org. Chem.* **1958**, 24, 1414–1419.
- (10) Frisch, M. J. et al. *Gaussian03, Revision C.02*; Gaussian, Inc.: Wallingford, CT, 2004 (for the full citation see the Supporting Information).
- (11) Takano, Y.; Houk, K. N. *J. Chem. Theory Comput.* **2005**, 1, 70–77.
- (12) (a) Cossi, M.; Rega, N.; Scalmani, G.; Barone, V. *J. Comput. Chem.* **2003**, 24, 669–681. (b) Klamt, A.; Schuurmann, G. *J. Chem. Soc., Perkin Trans.* **1993**, 2, 799–805. (c) Barone, V.; Cossi, M. *J. Phys. Chem. A* **1998**, 102, 1995–2001. (d) Cossi, M.; Barone, V.; Cammi, R.; Tomasi, J. *Chem. Phys. Lett.* **1996**, 255, 327–335.
- (13) McKee, M. L. *J. Phys. Chem. A* **2003**, 107, 6819–6827.
- (14) Camaioni, D. M.; Schwerdtfeger, C. A. *J. Phys. Chem. A* **2005**, 109, 10795–10797.
- (15) For recent applications, see: (a) Acevedo, O.; Jorgensen, W. L. *Org. Lett.* **2004**, 6, 2881–2884. (b) Acevedo, O.; Jorgensen, W. L. *J. Am. Chem. Soc.* **2005**, 127, 8829–8834. (c) Acevedo, O.; Jorgensen, W. L. *J. Org. Chem.* **2006**, 71, 4896–4902. (d) Acevedo, O.; Jorgensen, W. L. *J. Am. Chem. Soc.* **2006**, 128, 6141–6144.
- (16) (a) Jorgensen, W. L. *BOSS, version 4.6*; Yale University: New Haven, CT, 2004. (b) Jorgensen, W. L.; Tirado-Rives, J. *J. Comput. Chem.* **2005**, 26, 1689–1700.
- (17) Jorgensen, W. L.; Chandrasekhar, J.; Madura, J. D.; Impey, W.; Klein, M. L. *J. Chem. Phys.* **1983**, 79, 926–935.
- (18) Jorgensen, W. L. In *Encyclopedia of Computational Chemistry*; Schleyer, P. v. R., Ed.; Wiley: New York, 1998; Vol. 3, pp 1754–1763.
- (19) Repasky, M. P.; Chandrasekhar, J.; Jorgensen, W. L. *J. Comput. Chem.* **2002**, 23, 1601–1622.
- (20) Thompson, J. D.; Cramer, C. J.; Truhlar, D. G. *J. Comput. Chem.* **2003**, 24, 1291–1304.
- (21) Udier-Blagović, M.; Morales De Tirado, P.; Pearlman, S. A.; Jorgensen, W. L. *J. Comput. Chem.* **2004**, 25, 1322–1332.
- (22) (a) Tubert-Brohman, I.; Guimarães, C. R. W.; Repasky, M. P.; Jorgensen, W. L. *J. Comput. Chem.* **2004**, 25, 138–150. (b) Vayner, G.; Houk, K. N.; Jorgensen, W. L.; Brauman, J. I. *J. Am. Chem. Soc.* **2004**, 126, 9054–9058.
- (23) For prior studies of hydantoin tautomers, see: (a) Kleinpeter, E. *Struct. Chem.* **1997**, 8, 161–173. (b) Bausch, M. J.; David, B.; Dobrowolski, P.; Guadalupe-Fasano, C.; Gostowski, R.; Selmarten, D.; Prasad, V.; Vaughn, A.; Wang, L. H. *J. Org. Chem.* **1991**, 56, 5643–5651. (c) Bagno, A.; Comuzzi, C. *Eur. J. Org. Chem.* **1999**, 287–295. (d) Kleinpeter, E.; Heydenreich, M.; Kalder, L.; Koch, A.; Henning, D.;

Kempton, G.; Benassi, R.; Taddei, F. *J. Mol. Struct.* **1997**, *403*, 111–122.

Nascimento, M. A. C. *J. Phys. Chem. A* **1999**, *103*, 11194–11199.

- (24) For example, the equation  $\Delta G = -RT\ln K_a$  and a  $pK_a$  value of 9.03 gives  $\Delta G = 12.3$  kcal/mol. However, the free energy is increased by 2.4 kcal/mol to account for the concentration of liquid water. See: Da Silva, C. O.; Da Silva, E. C.;

- (25) Baboul, A. G.; Schlegel, H. B. *J. Chem. Phys.* **1997**, *107*, 9413–9417.

CT7001804